We are IntechOpen, the world's leading publisher of Open Access books Built by scientists, for scientists

6,900
Open access books available

185,000
International authors and editors

200M
Downloads

Our authors are among the

154
Countries delivered to

TOP 1%
most cited scientists

12.2%
Contributors from top 500 universities



WEB OF SCIENCE™

Selection of our books indexed in the Book Citation Index in Web of Science™ Core Collection (BKCI)

Interested in publishing with us?
Contact book.department@intechopen.com

Numbers displayed above are based on latest data collected.
For more information visit www.intechopen.com



9

Ion Conductive Polymer Electrolyte Membranes and Fractal Growth

Shahizat Amir, Nor Sabirin Mohamed and Siti Aishah Hashim Ali
University of Malaya
Malaysia

1. Introduction

It has been widely accepted that Euclidean geometry plays an important role in shaping the way natural forms are viewed in science and mathematics, arts and even the human psyche (Hastings & Sugihara, 1993). This happens because man always seeks to find simplicity and order in nature, and often makes approximation on natural forms that may be essentially complex and irregular. Hence, leaves are roughly ellipses, planets are spheres and spruce trees are cone-shaped. However, shapes such as coastlines, fern leaves and clouds are not easily described by traditional Euclidean geometry. Nevertheless, they often possess a remarkable invariance under changes of magnification. With a certain scale of magnification, the pattern is seen as repeating itself. Since the term 'fractal' was first coined by Mandelbrot (Mandelbrot, 1983), study of fractals has increasingly become an interest for scientists and mathematicians. Consequently many researchers study the growth and shapes of fractals through theoretical modeling and computer simulations of fractal patterns.

Simulation model of fractal patterns found in polymer electrolyte membranes provides another interesting perspective in the study of ion conductive polymer membranes. The characteristics and scientific aspects of the model have been studied and computer program s to simulate the growth of the patterns have been developed. Fractal aggregates especially diffusion-limited aggregate involve the random walk of particles and their subsequent sticking (Chandra & Chandra, 1994). To obtain fractal aggregates in laboratory framework, a system with particles in random walk is required. In most polymer electrolytes, the anions as well as the cations are found to be mobile and thus can be considered as a natural framework for fractal growth. The polymers act as a host while the inorganic salts dissociate in them to provide the ions necessary for conduction. According to Chandra (1996), fractals formed in the PEO-NH_4I polymer electrolyte films are principally due to the random walk and subsequent aggregation of iodine ions. In other research as well, Fujii et al. (1991) have successfully carried out fractal dimension calculations of dendrite, of fractal patterns observed on the surface of a conducting polymer polypyrrole, after an 'undoping' process. Recent studies of fractals in polymers that involved modeling and/or simulation include Janke & Schakel (2005), Lo Verso et al. (2006) and Marcone et al. (2007). On the other hand, Rathgeber et al. (2006) have done some work on theoretical modeling and experimental studies of dendrimers. There have also been experimental studies of crystal pattern transition from dendrites through fourfold-symmetric structures to faceted crystals of ultra thin poly(ethylene oxide) films which were carried out by Zhang et al. (2008). These research

works on fractals were done only on laboratory experiments, theoretical modeling and experimental studies, or modeling and computer simulations. Most recently, Amir et al. (2010a; 2011a) succeeded in integrating all the three approaches; experimental, modeling and simulation in studying fractals in different ion conductive polymer membranes (Amir et al., 2010a; 2010c; 2011a; 2011b). The study of fractal growth on ion conductive polymer membranes is useful in understanding the movement of ions in the films and can also be used to study heavy metal accumulation in diseased glands in humans and fishes (Chandra, 1996).

2. An overview of fractals

Benoit B. Mandelbrot (Mandelbrot, 1983) introduced the term 'fractal' that refers to a family of complex geometrical that can be characterized by a fractional or non-integer dimensionality. The concept of fractals has attracted the interest of scientists in many fields (Feder, 1988). A huge number of papers related to the word 'fractal' has been published, spanning fields ranging from physical geometry, such as surface structure of sea beds (Golubev et al., 1987), non-equilibrium growth phenomena (Shibkov et al., 2001) and distribution of intervals between earthquakes (Dargahi-Noubary, 1997), to ecology that involves fungal structure (Tordoff et al., 2007) and power law relationship between the area of a quadrate and the structure of peat systems (Sławinski et al.,2002). Even in cosmology with the study of the structure of star clusters and galaxies, the big bang theory of the origin of the universe and also in developmental biology portrayed by lung branching patterns, heart rhythms and structure of neurons (Hastings & Sugihara, 1993).

The most amazing thing about fractal is the variety of its applications. Besides theoretical applications, it can be used to compress data in the Encarta Encyclopedia and to create realistic landscapes in movies like Star Trek. The places where fractals can be found include almost every part of the universe, from bacteria cultures to galaxies and to human body. Many studies of fractals related to fields such as astronomy (Combes, 1998), biology (Stanley et al., 1994) and chemistry (Villani & Comenges, 2000). In mathematics, the study of fractals revolves around data compression, fractal art and diffusion.

Many of fractal growth models were also found to be suitable with experimental studies of electrochemical electrodeposition (Barkey, 1991), electrochemical polymerization (Kaufmann et al., 1987) and DLA growth structures of many metal aggregates in the presence of a magnetic field as external stimuli (Okubo et al., 1993). The formation of fractals without using any external stimuli has been reported by Chandra & Chandra (1993); Mohamed & Arof (2001) and Amir et al. (2010a; 2010c; 2011a; 2011b).

2.1 Fractal geometry

Fractal or fractional dimension is something that can never be understood inside the realm of elementary geometry. It is another field in which at least one of Euclid's postulates does not hold, and where other mathematical realities emerge. Thus, it can be said that there are two types of geometry: Euclidean and non-Euclidean geometries. In the first group, are the plane geometry, solid geometry, trigonometry, descriptive geometry, projective geometry, analytical geometry and differential geometry. In the second group, there are hyperbolic geometry, elliptic geometry and fractal geometry. Almost all geometric forms used for building man made objects belong to Euclidean geometry. They compromised of lines, planes, rectangular volumes, arcs, cylinders, spheres and defined shapes. These elements

can be classified as belonging to an integer dimension: 1, 2, or 3. Table 1 gives the summary of the major differences between fractal and the traditional Euclidean geometry.

EUCLIDEAN	NON EUCLIDEAN (FRACTAL)
Traditional (>2000 yrs)	Modern monsters (~ 30 yrs)
Based on characteristic size or scale	No specific scaling
Suits man made objects	Appropriate for natural shapes
Describes by formula	(Recursive) algorithm

Table 1. A comparison of Euclidean and fractal geometry (Peitgen & Saupe, 1988)

Fractal geometry allows length measurements to change in a non-integer or fractional way when the unit of measurements changes. The governing exponent D is called *fractal dimension* (Smith et al., 1990). The fractal dimension is a statistical quantity that gives an indication of how completely a fractal appears to fill space, as one zooms down to finer and finer scales. Fractal object has a property that more fine structure is revealed as the object is magnified, similarly like morphological complexity, which means that more fine structure (increased resolution and detail) is revealed with increasing magnification. Fractal dimension measures the rate of addition of structural detail with increasing magnification, scale or resolution. The fractal dimension, therefore, serves as a *quantifier of complexity*.

2.1.1 Self similarity

The main idea behind fractal geometry is self similarity. Self-similarity means that a structure (or process) can be decomposed into smaller copies of itself. This means that a self-similar structure is infinite. Self-similarity entails scaling. For an observable $A(x)$, which is a function of a variables x: $A = A(x)$, obeys a scaling relationship:

$$A(\lambda x) = \lambda^s A(x) \tag{1}$$

where λ is a constant factor and s is the scaling exponent, which is independent of x. For example, in a three-dimensional Euclidean space, volume scales as the third power of linear length, whereas fractals according to their fractal dimension (Focardi, 2003). Approximate self-similarity means that the object doesn't display perfect copies of itself. For example a coastline is a self-similar object, a natural fractal, but it does not have perfect self-similarity. A map of a coastline consists of bays and headlands, but when magnified, the coastline isn't identical but statistically the average proportions of bays and headlands remain the same no matter the scale (Judd, 2003).

It is not only natural fractals that display approximate self-similarity, the Mandelbrot set is another example. Identical pictures do not appear straight away, but when magnified, smaller examples will appear at all levels of magnification (Judd, 2003). *Statistical self-similarity* means that the degree of complexity repeats at different scales instead of geometric patterns. Many natural objects are statistically self-similar where as artificial fractals geometrically self-similar (Yadegari, 2003).

Geometrical similarity is a property of the space-time metric, whereas physical similarity is a property of the matter fields. The classical shapes of geometry do not have this property; a circle if on a large enough scale will look like a straight line. This is why people believed that the world was flat, the earth just looks that way to humans (Carr & Coley, 2003).

2.1.2 Fractal dimension

Fractal dimension is a measure of how complicated a self-similar figure is. In a rough sense, it measures how many points lie in a given set. The fractal dimension is often fractional. However, in algebra, the dimension of a space is defined as the smallest number of vectors needed to span that space (Rucker, 1984). In the 3 dimensional space, mathematicians traditionally denote the coordinates of three orthonormal vectors $\boldsymbol{x}$, $\boldsymbol{y}$ and $\boldsymbol{z}$. But sets are usually not vector spaces. Nevertheless, for aggregates, a fractal dimensionality in terms of scaling relationship between two different aggregate's properties X and Y (e.g. mass and length) can be observed such as (Meakin, 1988):

$$Y \propto X\ d_f \tag{2}$$

where d_f is all purpose fractal dimension as described by Meakin (1988).
Mandelbrot (1983) developed the 'concept of homothetic dimension' relative to geometric fractals. Let X be a complete metric space and let $A \subset X$. If N (A, ϵ) is the least number of balls of radius less than ϵ that are needed to cover A, then the number D (A) defined by

$$D(A) = \lim_{\varepsilon \to 0} \frac{ln\, N(A, \varepsilon)}{ln \frac{1}{\varepsilon}} \tag{3}$$

and is called the fractal dimension of A.
For each part (N) of the fractal deducted from the whole and having a homothetic ratio $r(N)$, the fractal dimension d_f is defined as:

$$d_f = \frac{Log(N)}{Log\left(\frac{1}{r}\right)} \tag{4}$$

For example, the Von Koch's snowflake iteration as illustrated in Figure 1, each side of unit 1 of a triangle is divided by 3, hence. $r = 1/3$. The central third of one side is replaced by 2 smaller lines of length 1/3. Therefore, one line is now subdivided in 4 smaller lines of length 1/3, hence. $N = 4$. Its fractal dimension now becomes:

$$d_f = \frac{Log(4)}{Log(3)} \approx 1.262 \tag{5}$$



Fig. 1. Construction of the Von Koch's snowflake

2.1.3 Types of fractals

Fractal geometry is the geometry of structures that have a scaling symmetry. The simplest types of fractals are self-similar fractals that are invariant to an isotropic change of length scale (Meakin, 1991). Another approach to fractals is the way they are generated, for example by an *iterative* process. This process of iteration leads to different categories of fractals. Generally fractals can be divided into two main categories:

1. Deterministic Fractals
2. Random Fractals

2.1.3.1 Deterministic fractals

Deterministic fractals are generated by an iterative process. The term deterministic means that a simple process of iteration is applied to build the fractals such as the iteration of a complex function that generates the 'Mandelbrot Set' as shown in Figure 2. The iteration process is a geometrical transformation called *generator* on an object. This object is called *initiator*. For the construction of the so-called 'Koch's Curve' the transformation for each iteration is repeated. To build this fractal, a line of unit 1 is divided by 3 and the central $\frac{1}{3}$ is taken out and is replaced by 2 lines of length $\frac{1}{3}$. On the next iteration, the same transformation is applied on the remaining lines repeatedly. Its construction is described in Figure 2 as follows:

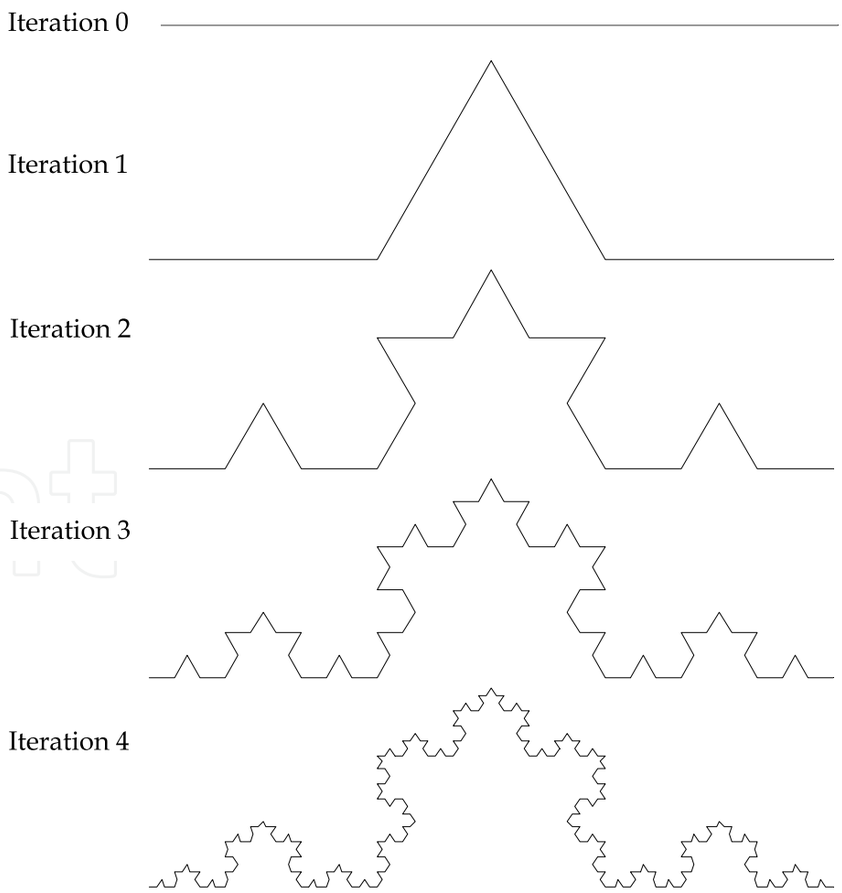


Fig. 2. Construction of Koch's curve (Addison, Paul S., 1997)

An important property of this fractal is its length that is infinity. The length of the initiator is 1, therefore, after the first iteration; the calculated length of the object is 4 lines of length $\frac{1}{3}$, that is $\frac{4}{3}$. Then the second iteration gives 16 lines of length $\frac{1}{9}$. The length now becomes equal to $\frac{16}{9}$. More generally, at each iteration n, the length becomes equal to $(4/3)^n$. As n tends to infinity, the length is $(4/3)^{\infty} = \infty$. The property of self-similarity can also be easily seen, as illustrated in Figure 3.

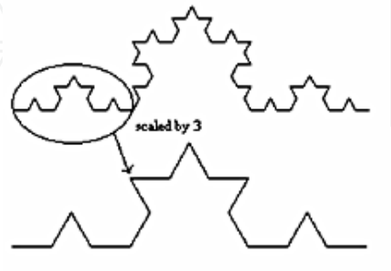


Fig. 3. Self similarity property of the Koch Curve

2.1.3.2 Random fractals

Random fractals are generated by stochastic processes, for example, trajectories of the Brownian motion, Lévy flight, fractal landscapes and the Brownian tree. The latter yields the so-called mass- or dendritic fractals, for example, diffusion-limited aggregation clusters. In the 1980's, Meakin developed different aggregation models in order to study the various ways an aggregate could be generated (Meakin, 1988; Meakin, 1991). Those aggregation models which are similar to the L-system are computer-generated where a set of transformation is applied on the generator that, in this case, would be an initial particle or cluster in the model. Random fractals have been used extensively in computer graphics to model natural objects (Ebert, 1996).

Many attractive images and life-like structures can be generated using models of physical processes from areas of chemistry and physics. One such example is diffusion limited aggregation (DLA) which describes, among other things, the diffusion and aggregation of zinc ions in an electrolytic solution onto electrodes. 'Diffusion' is because the particles forming the structure wander around randomly before attaching themselves (aggregating) to the structure. 'Diffusion-limited' because the particles are considered to be in low concentrations so they do not come in contact with each other and the structure grows one particle at a time rather then by chunks of particles. Other examples can be found in coral growth, the path taken by lightning, coalescing of dust or smoke particles, and the growth of some crystals.

2.2 Significance of fractals

The term fractals have always been associated with the complex geometric shapes which can be characterized by non-integer dimensions. Generally, fractals can be found in unbalanced phenomena either naturally or experimentally developed in laboratories. The fractal concept has been used in many fields like chemistry, biology, medicine, weather forecast and engineering where it provides understanding of the extraordinary patterns and chaos (Radnoczy et al., 1987; Chandra & Chandra 1996; Neimeyer et al., 1984).

2.2.1 Fractals in physical sciences

Fractals obviously generate some convincing models of natural phenomena such as mountains and clouds for use in computer graphics imagery, and they provide very compelling abstract pictures. But since 1980's until 1990's, about one third of all physics papers submitted to journals for publication at least mentioned fractals somewhere (Musgrave, 1993). It is also known that many universities all around the world have now offered courses on the subject fractals mainly concerning the field of mathematics and physics.

Looking at fractals in mathematics, some fractal patterns exist only in mathematical theory, but others provide useful models for the irregular yet patterned shapes found in nature such as the branching of rivers and trees. Mathematicians tend to rank fractal dimensions on a series of scales between 0 and 3. One-dimensional fractals (such as a segmented line) typically rank between 0.1 and 0.9, two-dimensional fractals (such as a shadow thrown by a cloud) between 1.1 and 1.9, and three-dimensional fractals (such as a mountain) between 2.1 and 2.9. Most natural objects, when analyzed in two dimensions, rank between 1.2 and 1.6 (Ouellette, 2001).

The nonlinear mathematics models nature more accurately, but is intractable in comparison to the linear approximations. When computers made it possible for scientists to begin to cope with these previously-intractable nonlinear systems, they discovered something very surprising which is in any perturbation to the initial state of the system, no matter how small or seemingly insignificant, will cause the system to diverge; that is to evolve into an arbitrarily different future state, within a finite period of time. This discovery is known as *deterministic chaos* or *sensitivity to initial conditions*.

2.2.2 Fractals in biological sciences

Biologists have traditionally modeled nature using Euclidean representations of natural objects or series. Examples include the representation of heart rates as sine waves, conifer trees as cones, animal habitats as simple areas, and cell membranes as curves or simple surfaces. However, scientists have come to recognize that many natural constructs are better characterized using fractal geometry. Biological systems and processes are typically characterized by many levels of substructure, with the same general pattern being repeated in an ever-decreasing cascade. Relationships that depend on scale have profound implications in human physiology (West & Goldberger, 1987), ecology (Loehle, 1983; Wiens, 1989), and many other sub-disciplines of biology. The importance of fractal scaling has been recognized at virtually every level of biological organization.

Fractal geometry may prove to be a unifying theme in biology (Kenkel & Walker, 1993) since it permits generalization of the fundamental concepts of dimension and length measurement. Most biological processes and structures are non-Euclidean, displaying discontinuities, jaggedness and fragmentation. Classical measurement and scaling methods such as Euclidean geometry, calculus and the Fourier transform assume continuity and smoothness. However, it is important to recognize that while Euclidean geometry is not realized in nature, neither is strict mathematical fractal geometry. Specifically, there is a lower limit to self-similarity in most biological systems, and nature adds an element of randomness to its fractal structures. Nonetheless, fractal geometry is far closer to nature than is Euclidean geometry (Deering & West, 1992).

The relevance of fractal theory to biological problems is dependent on objectives. To the forester interested in estimating stand board-feet, a Euclidean representation of a tree trunk

(as a cylinder or elongated cone) may be quite adequate. However, for an ecologist interested in modeling habitat availability on tree trunks (say, for small epiphytes or invertebrates), fractal geometry is more appropriate. Using the approach of fractal geometry, the complex surface of tree bark is readily quantified.
A forester's diameter tape ignores the surface roughness of the bark, giving but a crude estimate of the circumference of the trunk. For an insect 10 mm in length, the distance that it must travel to circumnavigate the trunk is much greater than the measured diameter value. For an insect of length 1 mm, the distance traveled is even greater. This has consequences on the way that the tree trunk is perceived by organisms of different sizes. If the bark has a fractal dimension of $D = 1.4$, an insect an order of magnitude smaller than another perceives a length increase of $10^{D-1} = 10^{0.4} = 2.51$, or a habitat surface area increase of $2.51^2 = 6.31$. By contrast, for a smooth Euclidean surface, $D = 1$ and both insects perceive the same 'amount' of habitat. The higher the fractal dimension D, the greater the perceived rate of increase in length (or surface) with decreasing scale.

2.3 Fractal growth models

Many fractal growth phenomena found in experiments and numerical simulations explored the properties of aggregation kinetics, gelation, and sedimentation (Aharony, 1991). The aggregation of particles often produces fractal clusters. A typical aggregate is the commonly known computer generated simulation of ‘diffusion limited aggregation’. The shape looks very similar to those arise in many natural aggregation processes, including diffusion limited electrodeposition (Matsushita et al., 1984), growth in aqueous solutions (Sawada et al., 1986), dielectric breakdown (Niemeyer et al., 1984), viscous fingers in porous media (Maloy et al., 1985), and fungi and bacterial growth (Matsuura & Miyazima, 1992; Matsuyama et al., 1993; Ben-Jacob et al., 1994).
To describe these aggregates, one must first characterize their structures quantitively (Aharony, 1991). Characterization on its fractal dimensionality, or exponents, each of which determines one of its physical properties is very important. Growth models are used to understand the relationship between the microscopic interactions which are responsible for its growth, and the specific complex macroscopic shapes. This is done by setting up a few simple microscopic growth rules, by which particles are added to the aggregate and with repeated iteration it gives rise to the macroscopic cluster. Some of the well known fractal growth models normally used for simulation of fractals are described in the following sections.

2.3.1 Eden model

The Eden model is the simplest growth model (Eden, 1961) and the one that probably applies in most cases. Starting from an initial seed, a new particle is added to cluster on one of the surface sites. A surface site here is defined as a site sharing a side with the existing cluster. The way in which the surface site is chosen can vary. One version of the Eden model selects with equal probability among all the surface sites where a new particle will be added. Another version counts the number of neighbors of each surface site and the probability that a new particle is added is directly proportional to the number of neighbors. The third version of the Eden model chooses a ’mother cell’ with equal probability among the particles which are not completely surrounded by other particles.

2.3.2 Percolation model

The randomness of a fluid spreading through a medium maybe of two quite different types (Feder, 1988). The first type is the random walks of the fluid particles in the familiar diffusion processes. The other case in which the randomness is frozen into the medium itself and it is known as a 'percolation process', since it behaves like coffee in a percolator (Broadbent & Hammersley, 1957).

Compared to diffusion process where a diffusing particle may reach any position in the medium, percolation process has a feature, where there exists a 'percolation threshold', under which the spreading process is confined to a 'finite' region. For example, spreads of blight from one tree to the other in an orchard where the trees are planted on the intersections of a square lattice. Here, when the spacing between the trees is increased so that the probability for infecting a neighboring tree falls below a critical value, then the blight will not spread over the orchard. Thus, the value of the percolation threshold has to be determined by simulations.

2.3.3 Ballistic deposition model

Ballistic deposition was introduced as a model of colloidal aggregates, and early studies concentrated on the properties of the porous aggregate produced by the model (Family, 1990: Horvath et al., 1991). The particles in the ballistic deposition model follow a straight-line trajectory until they first encounter a particle on the surface, or a particle in one of the nearest-neighbor columns. As soon as a particle reached such a position, it permanently sticks to the surface and becomes part of the deposit. Evolution of an interface in a ballistic deposition model can be described by the dynamic scaling approach (Family & Vicsek, 1985). Moreover the surface of the deposit is a self-affine fractal, since the atoms are not allowed to diffuse on the surface.

2.3.4 Dielectric breakdown model

Dielectric breakdown refers to the formation of electrically conducting regions in an insulating material exposed to a strong electric field. For example, the intense electric fields during thunderstorms can produce a conducting path in the air along which many electrons flow (lightning). A formal model, ignoring the physical details of the processes, was proposed in 1984 by Niemeyer, Pietronero and Weismann (Niemeyer et al., 1984). Dielectric breakdown patterns exhibit a branching, fractal pattern with a dimension of about 1.7.

2.3.5 Viscous fingering model

In viscous fingering the principal force is due to viscous forces in the defending fluid (Aharony, 1991). The process is obtained by injecting a low viscosity fluid into a medium of high viscosity fluid with a high injection rate. The capillary effects and the pressure drop in the invading fluid are negligible. The structures typically consist of fingers of invading fluid that propagate through the medium with only a few small trapped clusters of defending fluid left behind. Viscous fingering was first studied in a Hele-Shaw channel where one observes fingering patterns when glycerol is displaced by air (Saffman & Taylor, 1958). A Hele-Shaw cell consists of two transparent plates separated by a given distance and the patterns obtained are fully described by Darcy's equation and the capillary pressure due to the interfaces between the two phases. In 1985, Chen and Wilkinson (Chen & Wilkinson, 1985) and Måløy and coworkers (Måløy et al., 1985) studied viscous fingering in a porous

medium where they concluded that the disorder of the system has significant effect on the fingering process.

2.3.6 Diffusion limited aggregation model

Diffusion limited aggregation (DLA) is a model of irreversible growth to generate fractal structures as proposed by Witten and Sander (1981). It has been used to study a great variety of processes including dendritic growth, viscous fingering in fluids, dielectric breakdown and electrochemical deposition. The model is set by the following simple rules:

A seed is fixed at the origin of some coordinate system and one particle is released from a far-away boundary and allowed to take random walks (diffuse). If the particle touches the seed, it irreversibly sticks to the seed and forms a two-particle aggregate. As soon as the random walker is removed either by being captured or escaping the boundary, the next walker is released and the process is repeated. Now it can stick to any particle in the aggregate as well as the original seed.

The resulting clusters are highly branched since DLA enhances the instability of growth. The arriving particles are far more likely to stick to the tips of outer branches than to maneuver their way deep into the *fjords* (narrow inlet of a section) before contacting the surrounding branches. Thus the tall branches of the cluster screen the small ones and grow faster. The growth on the tips, however, is not always in the outward radial direction. Sometimes a few new branches are spun off from one tip site as occurred in the original seed. The *tip-splitting* makes the DLA clusters a self similar fractal.

2.4 Methods for determination of fractal dimension

Fractal dimension is a statistical quantity that gives an indication of how completely a fractal appears to fill space, as one zooms down to finer and finer scales. There are many specific definitions of fractal dimension. Summary of some of the more commonly used methods for determination of fractal dimension of natural forms are presented in this section. These methods include the information dimension method, mass dimension method and box counting method.

i. Information dimension method

This method requires the use of boxes but is generally different from the box counting method. It does not consider the number of boxes occupied regardless of whether it contains one point of relatively large number of points. Instead, the information dimension effectively assign weights to the boxes in such a way that boxes containing a greater number of points count more than boxes with fewer points (Dierking, 2000). The fractal dimension D_i is given from the proportionality

$$I(d) \sim -D_i \log(d) \tag{5}$$

with $I(d)$ is the information entropy of $N(d)$ boxes of size d, given by

$$I(d) = -\sum_{i=1}^{N(d)} m_i \log(m_i) \tag{6}$$

with $m_i = \frac{M_i}{M}$ where M_i is the number of points in the ith box and M the number of total points in the data set.

ii. Mass dimension method
The mass dimension method also known as the Scholl method, which yields the fractal dimension D_m, following the proportionality

$$m(r) \sim r^{Dm} \tag{7}$$

where $m(r) = M(r)/M$ is the 'mass' within a circle of radius r, where $M(r)$ is the data set of points contained within a circle and M the total number of points in the set. If the set is a fractal, the plot of log $m(r)$ versus log r will follow a straight line with a positive slope equal to D_m (Dierking, 2000). This method is best suited to objects that follow some radial symmetry, such as the dendritic growth in radial axis.

iii. Box-counting dimension
In fractal geometry, the box-counting dimension is a way of determining the fractal dimension of a set S in a Euclidean space R^n. To calculate this dimension for a fractal S, imagine this fractal lying on an evenly-spaced grid, and count how many boxes are required to cover the set. The box-counting dimension is calculated by seeing how this number changes as the grid becomes finer.
Suppose that $N(s)$ is the number of boxes of side length s required to cover the set (Hastings & Sugihara, 1993), then S has box dimension D if $N(s)$ satisfies the power law

$$N(s) \approx c(1/s)^D \tag{8}$$

asymptotically in the sense that

$$\lim_{s \to 0} N(s) s^D = c \tag{9}$$

By solving equation (8) asymptotically for D, the box-counting dimension is computed as:

$$D = \lim_{s \to 0} \left[-\frac{\log N(s)}{\log s} \right] \tag{10}$$

This method is a favorite among most researchers and is considered the easiest to perform (McNamee, 1991). The box-counting dimension can be used to analyze irregularities in surfaces filling space volume and suitable for images, however complex. The use of a mesh grid overlapped over a structure allows the box counting method to conduct both textural and structural analysis of a structure. In addition, the mesh grid also allows the analysis of objects scattered in an image and this method can be adapted to measure objects or processes in multiple dimensions (Cross, 1997).

3. Simulation of fractals

3.1 Simulation of fractals using DLA model

DLA is one of the most important models of fractal growth. This model is based on the Brownian motion theory. It refers to a simple growth algorithm in which individual particles are added to a growing cluster through diffusion-like process. Starting from any suitable immobile aggregate seed in a plane, a new particle is launched at a random position far away from the aggregate seed and is allowed to undergo Brownian motion. When the random walking particle touches the seed, it is stopped and incorporated to the aggregate.

The process of launching a random walker and adding it to the aggregate on its first contact is repeated until the aggregate reached a desired number of particles (Witten & Sander, 1981). Figure 4 gives a visual representation of the above mentioned process.

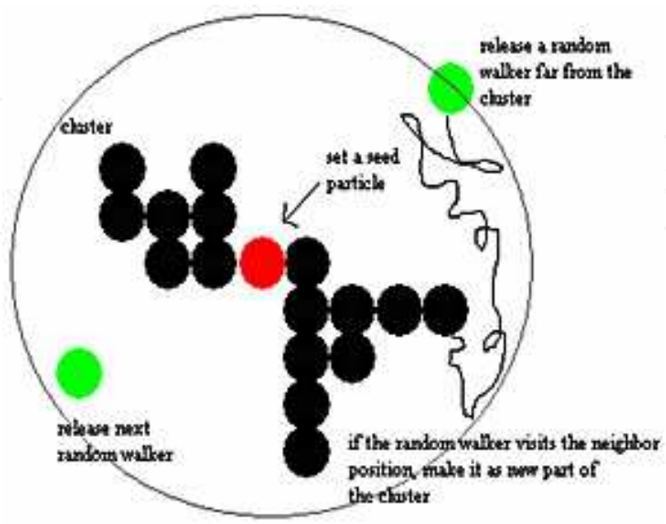


Fig. 4. An off the scale model of aggregation of cluster particles

3.2 Simulation of fractal pattern using a grammar based model (L-systems)

L-systems; a mathematical formalism as a foundation for an axiomatic theory of biological development **(**Lindenmayer, 1968) was proposed by a biologist, Aristid Lindenmayer in 1968. L-systems have found several applications in computer graphics especially in areas which include generation of fractals and realistic modeling of plants. Central to L-systems, is the notion of rewriting, where the basic idea is to define complex objects by successively replacing parts of a simple object using a set of rewriting rules or productions. The rewriting can be carried out recursively.

Aristid Lindenmayer's L-systems introduced a new type of string rewriting mechanism. In L-systems, grammars productions are applied in parallel, replacing simultaneously all letters in a given word. There are a number of different types of L-systems. The two major classifications are reflected in the naming conventions:

1. Deterministic
2. Stochastic

The two classes of L-systems make it possible to generate simple and complex geometric patterns in the study of fractals.

3.2.1 Deterministic L-systems

Also known as D0L-systems, deterministic L-system is the simplest classes of L-systems. D0L stands for deterministic and 0-context or context-free L-systems. The rewriting process starts from a distinguished string or initiator called the axiom, and followed by a generator (rules) that is applied to the axiom to generate a new string. This generation can be iterated to produce strings of arbitrary length, which then can be interpreted as a series of turtle commands by a turtle graphic system (Abelson & diSessa, 1982). This turtle concept is explained in detail in section 3.2.3.

3.2.2 Stochastic L-systems

L-systems are usually deterministic and they provide description based on individual patterns. Consequently, every time a word is derived using a given system, the resulting words will be the same (Prusinkiewicz & Lindenmayer, 1990). This may lead to restrict a certain pattern to a certain form and would not always be desired. Imagine visualizing complex fractal patterns found in many natural processes, such as electrodeposition, growth in aqueous solutions, dielectric breakdown, viscous fingers in porous media, and fungi and bacterial growth. If only one L-System was used to describe every pattern, then the results would look unrealistic (Kaandorp, 1994). On the other hand, creating a single L-System with individual productions for each pattern would be a tedious task, and it still could not guarantee similarity between individuals.

Instead of using only one L-system to describe these patterns, it is wiser to use probabilistic/stochastic L-Systems. Each of these production/rules is assigned a probability. All fractal growth patterns generated by the same deterministic L-system are identical. An attempt to combine them in the same picture would produce a striking, artificial regularity (Prusinkiewicz & Lindenmayer, 1990). In order to prevent this effect, it is necessary to introduce one-to-one variations that will preserve the general aspects of a pattern but will modify its details. Variations can be achieved by randomizing the turtle interpretation, the L-system, or both.

In order to achieve this, it is necessary to use suitable production rules with the implementation of the turtle graphics command in a turtle graphics system. Stochastic L-Systems was considered a more suitable simulation technique for the simulation of fractals formed without using any external stimuli.

3.2.3 Graphical representation of L-systems

The most common turtle interpretation used in L-system today is based on the LOGO-style turtle (Abelson & diSessa, 1982), as introduced by Prusinkiewicz (1986). The main concept is that some modules in the L-system string are interpreted as commands executed by a turtle. In 2D, the *state of the turtle* (S) is characterized by its position and orientation. Turtle graphic interpretations can exhibit different levels of complexity (Alfonseca & Ortega, 2001). Papert (Papert, 1980) created turtle graphics in 1980, describing it as a trail left by an invisible 'turtle' whose state at every instant is defined by its position and the direction in which it is looking. Set of instructions (commands) to the turtle (Peitgen et al., 1992) are explained as follows:

- F moves the turtle one step forward, in the direction of its current angle, leaving a visible trail. We call F a 'draw 'letter.
- *f* moves the turtle one step forward, in the direction of its current angle, with no visible trail.
- +(plus) increases the turtle angle by θ.
- -(minus) decreases the turtle angle by θ.
- [stacks the current position and orientation of the turtle.
-] moves the turtle invisibly to the position and orientation stacked at the top of the stack and pops it.

A state of the graphic turtle is defined as a triplet (x, y, θ), where the Cartesian coordinates (x, y) represent the turtle's position in 2D space, and the heading, the angle θ is interpreted as the direction in which the turtle is heading.

The following is an example of an L-system specification.

Axiom: F
Production rules: F → F[+F]F[-F] [F]
Angle, θ:30^o

Derivation of a string from an L-system is done in much the same way that a string is formed from a traditional grammar. It begins with the axiom, F. At any point in the derivation, all Fs in a string are replaced in parallel by a particular replacement string. In the L-system described above, each F in a string is replaced by F[+F]F[-F] [F] . So, starting with the axiom, F, the string after one substitution would be

F[+F]F[-F] [F]

and the string after two substitutions would become

F[+F]F[-F] [F] [+F[+F]F[-F] [F]]F[+F]F[-F] [F] [-F[+F]F[-F] [F]][F[+F]F[-F][F]]

A generated object is often referred to by the number of string substitutions that has been performed. The numbers of iterations are defined as being one greater than the number of string substitutions. Figure 5 illustrates the objects for four different iterations that have been generated from the L-system described above.

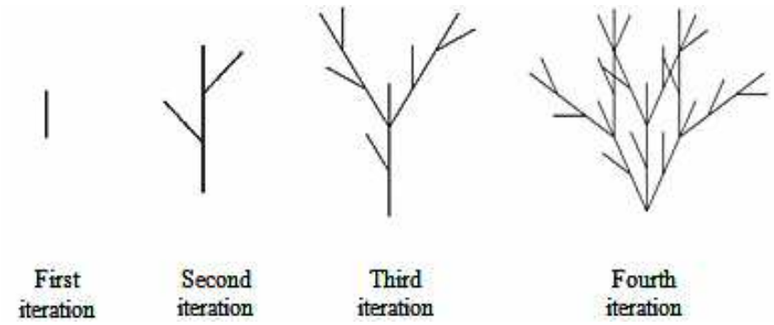


Fig. 5. Objects generated from an L-system until the fourth iteration

4. Fractals in ion conductive polymer electrolytes

Eversince the introduction of the 'Fractal Geometry' concept by Mandelbrot (Mandelbrot, 1983) in 1977, much work was concentrated on theoretical simulation/modeling of this concept. Theoretical simulation of fractal patterns, in particular Diffusion Limited Aggregate (DLA) requires particles of uniform as well as non-uniform size performing random walk. In the case of polymer electrolyte membranes, studies have been done to develop polymer electrolytes with high ionic conductivities especially in the field involving advanced materials known as superionic solids or fast ionic conductors (Amir et al., 2010b). In this type of conductors, the conductivity is due to the motion of ions. Superionic solids or fast ionic conductors brought about the development of high energy density batteries (Armand et. al, 1979; Murata, 1995; Borghini et. al, 1996), electrochomic devices (Ratner, 1987; Scrosati, 1990), fuel cells (Prater, 1990), chemical sensors (Somov et. al, 2000) and capacitors (Pernaut and Goulart, 1996) etc. Initially, the fractals observed in the polymer electrolytes were discovered by chance. Some of the fractals observed in the polymer electrolyte membranes are shown in Figures 6(a)-(c). The study of these fractals may be useful in understanding the movement of ions in the polymer electrolyte membranes.

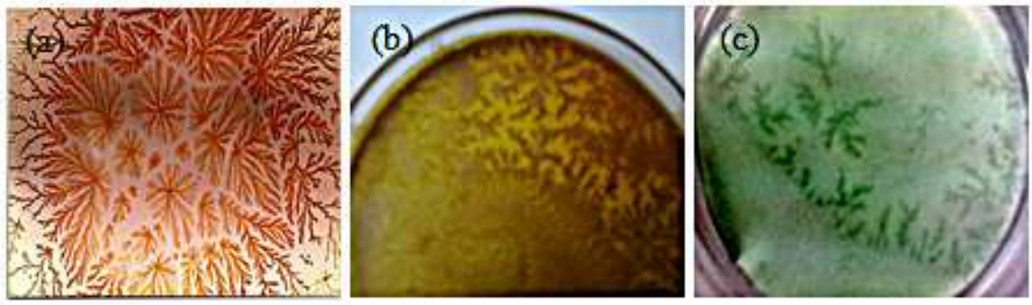


Fig. 6. Fractal aggregates of different sizes in (a) chitosan (b) PEO and (c) PVDF-HFP based electrolyte membranes

4.1 Fractal growth patterns identification and simulation

It has been identified that the formation of fractals without using any external stimuli resulted into isotropic DLA patterns as reported by Chandra (1996) and Amir et al. (2010a; 2011b). Amir et al. (2010a; 2011a; 2011b) have succeeded to obtain fractal aggregates of different sizes in the films such as PEO, chitosan and PVDF-HFP polymers infused with an inorganic salt without any external stimuli. As can be observed in Figure 6, fractals are formed at the different nucleation centers and then grow in certain directions away from the nucleation site. The fractals grow irregularly and in an unpredictable motion. Among the techniques used to simulate such fractal patterns are DLA model which is based on the Brownian motion theory and fractal dialect called L-systems.

4.2 Simulation of fractals in ion conductive polymer membranes

Simulation of the DLA model gives a simple yet effective way to represent fractals obtained in polymer membranes. On the other hand, the simulation using the L-system technique provides a general approach on how to visualize growth of fractals with respect to the production rules involved and the governing number of iterations required to actually simulate a model that best represent the original pattern observed in the experimental outcome.

4.2.1 Simulation using DLA model on a square lattice

Computer simulations of the fractals are performed based on the DLA model described earlier. The simulation starts with a single seed at the centre of a square lattice. Then the seed will start to grow gradually until a full single cluster is formed. This cluster grows outward, one generation after another. The basic algorithm of the whole process is as follows:

1. A list called **occupiedSites** is created, containing the lattice site {0, 0}.
2. Determine the lattice site nearest to a randomly chosen location along the circumference of a circle whose radius, rad, equals a specified value, s, plus the maximum absolute coordinate value in **occupiedSites**.
3. Starting at the selected lattice site, execute a lattice walk until the step location is either at a distance greater than (rad + s), or on a site that is contiguous (adjacent) to a site in **occupiedSites**. Call the final step location of the walk, **loc**.
4. Check if **loc** is adjacent to a site in the occupiedSites list and if it is, add loc to occupiedSites.
5. Execute the sequence of steps 2 through 4 until the length of **occupiedSites** reaches a value *n*.

Figure 7 gives an illustration of the implementation of the DLA algorithm.

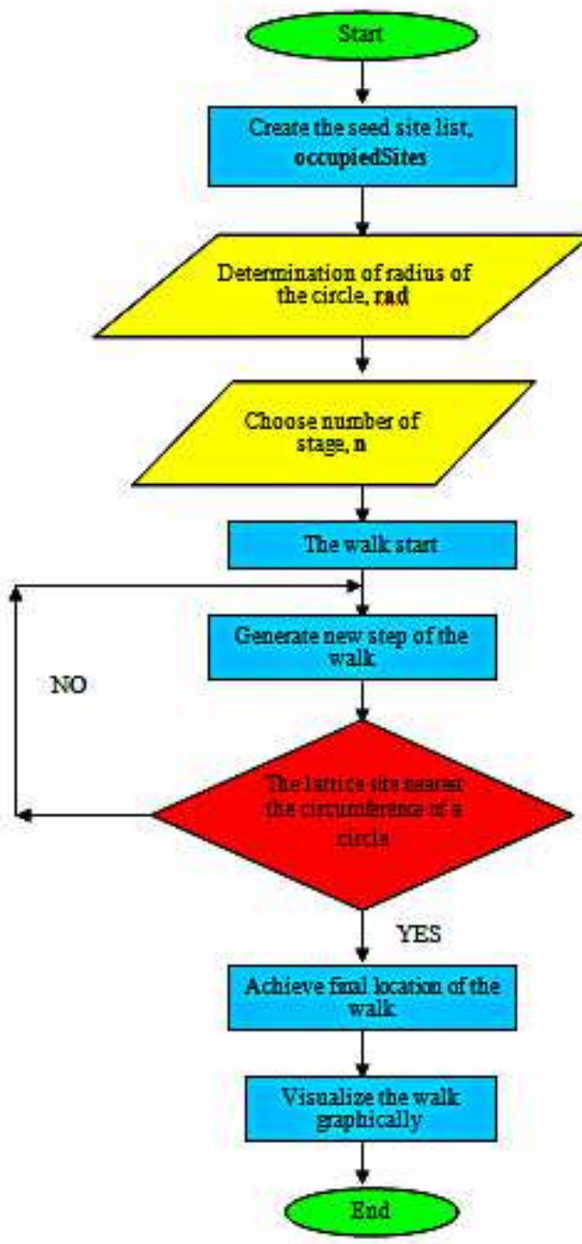


Fig. 7. An illustration of the simulation of DLA model on a square lattice

In summary, the algorithm adds a particle as a result of random walk of a drifter from the perimeter to a point on the boundary of the structure. The drifters were introduced into the grid at a point chosen at random from the points equidistant from the origin, where the initial particle was placed. If the movement of a drifter would take it beyond this perimeter, it is reflected back to the interior. If it moves to a point on the boundary of the structure, it is transformed into a part of the structure. This process is repeated until the desired stage has been achieved.

For simulation purposes, the images of the fractal patterns such as those displayed in Figure 8 are chosen specifically.



Fig. 8. DLA fractals in a PEO-NH_4I membrane

The simulation of the fractal patterns can be carried out on a square lattice. The animation for a single cluster of the pattern can be created using a computer program developed in order to show how the cluster grows starting from the original nucleation centers that eventually grow according to a specific size desired. There are some properties of the clusters that have been identified. These properties are as follows:

1. Branching and screening
   The random growth process leads to the formation of small tips which are likely to capture diffusing particles. They *screen* their surroundings which later have the effect of screening that will *self-stabilize* the tip until it grows even larger forming new tips which are delicate, branched and tree–like objects.
2. Scale invariance, lack of a typical length-scale
   As the stage of growth increases, it seems like they are a hierarchy of arms, branches, twigs and sprouts with *fjord* like empty regions of all sizes.
3. Stochastic self–similarity
   Substructures of the cluster are found to be self-similar i.e. they can be reproduced after proper rescaling.

Apart from the identified properties of the DLA cluster, it is also important to know the growth site probabilities for every particle released during the simulation. It has been discovered that diffusing particles are highly unlikely to wander into one of the inner *fjords.* The diffusing particles have a high probability to attach to the protruding tips. They are already visible from the marking of most recent particles and growth occurs essentially only in a small *active zone* within the predetermined radius.

Figures 9(a) (i-v) present the fractals of PEO-NH_4I (60:40 wt %) membrane as observed in figure 8. Their patterns simulated using DLA model are shown in Figures 9(b) (i-v).

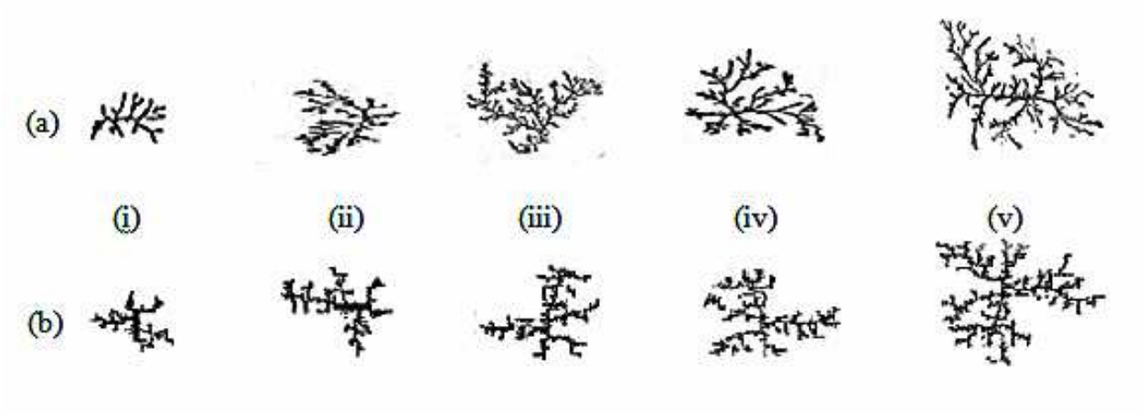


Fig. 9. The experimentally observed (a) and simulated (b) DLA patterns in PEO-NH_4I system using DLA model

The fractal dimensions for the simulated and cultured fractals are listed in Table 2. The fractal dimensions of the cultured fractals are determined using a computer software tool, utilizing the box-count method, developed by Suki et. al. (2007) while those of simulated fractals are calculated automatically by a subprogram incorporated in the simulation program. The table shows that the fractal dimension values of the simulated fractals are comparable with the fractal dimension values obtained from their respective experimentally cultured ones. For example, the fractal dimension of experimentally cultured fractal in Figure 9(a) (v) is 1.742 ± 0.044 while its corresponding simulated fractal, Figure 9(b) (v) has a fractal dimension of 1.778 ± 0.043. In every calculation of the fractal dimension, the error values for both experimentally and simulated patterns are found to be so small with standard deviation of less than 1.6%.

Experimentally cultured fractals		Simulated fractals using DLA model		Percentage of difference (%)
Figure	Fractal dimension	Figure	Fractal dimension	
9(a)(i)	1.688 ± 0.049	9(b)(i)	1.725 ± 0.044	1.29
9(a)(ii)	1.719 ± 0.043	9(b)(ii)	1.765 ± 0.049	1.56
9(a)(iii)	1.754 ± 0.047	9(b)(iii)	1.759 ± 0.042	0.16
9(a)(iv)	1.706 ± 0.045	9(b)(iv)	1.747 ± 0.045	1.41
9(a)(v)	1.742 ± 0.044	9(b)(v)	1.778 ± 0.043	1.19

Table 2. Fractal dimension values of the fractals simulated using DLA model and their respective experimentally cultured fractal patterns.

From the table, it is clear that the percentage difference of fractal dimension values between the experimental and simulated patterns are marginally close. The highest percentage difference is found to be less than 1.6% that is 1.56%. The lowest percentage difference is 0.16%. These show that the simulated fractal patterns were of fairly good conformity with the fractal patterns observed in the PEO-NH_4I polymer films.

The small difference of fractal dimension values between the experimental and simulated patterns maybe attributed to the way the simulation was done in the simulation. The

simulation of fractal patterns using the modeling of DLA on a square lattice written in a computer program chosen for this study has a run time restriction. To actually simulate a larger fractal pattern requires a longer time to complete as a particle that moves close to the cluster has to investigate all neighbor sites, whether these already belong to the cluster. The particle should either stick or walk freely. The information about the neighborhood should be assigned to each site, so that a walker only make contact with the site which it is on instead of all four (in a square lattice) possible neighbors.

4.2.2 Fractal growth simulation using L-systems

Stochastic L-system allows various shapes to be drawn. The recursive nature of the L-system rules leads to self-similarity and thereby complex geometric patterns which are easy to describe with an L-system. The rules of the L-system grammar are applied iteratively starting from the initial state which is called the axiom and a set of production rules.

To develop an L-system for a particular simulation of the complex geometric patterns, some steps (Hashim_Ali et al., 2000) have to be followed:

i. the fractals must be analyzed to infer its stages of growth.
ii. define the axiom and production rules into a string of symbols that assigned a particular meaning.
iii. execute the rules as a computer program and show the results as a graphical output and calculate its fractal dimension.
iv. compare the simulation with the real patterns obtained in the polymer membranes.

As observed in Figure 8, the fractal patterns found in polymer electrolytes take on a branching structure. The branching structure is represented by the square bracket symbols (refer section 3.2.3). When a branch point is reached, the turtle encounters the left square bracket '[' where it should remember its current position and heading. This is called the state of the turtle. Technically the state S is given by $S = \{x, y, \theta\}$. In mathematical terms, the turtle has a state consisting of its current position, given by two coordinates x and y, and a current heading, specified by an angle θ. On the other hand when the turtle reaches the corresponding closing bracket ']' the commands are terminated and the turtle will then return to the branching point which it must remember. In the analysis of fractal growth patterns, there are a few important factors to be considered in performing the simulation. The main criterion is the structure of the fractal such as the number of branches, the size of the structure, and most of all the production rules that suit the original pattern. For the fractals shown in Figure 8, to achieve a good result, three key components in the simulation were identified. They are as follows:

i. Generally, the numbers of branches in most of the observed fractal patterns are about four.
ii. The size of the object differs from one to the other but to obtain the best model for the structure; when running the simulation, the stage of iteration should be at least six. The purpose of choosing the stage of iteration is because if the stage of iteration was too low or too high, it would be hard to get a generally satisfying model for the structure. This is to ensure a 'mature' fractal growth pattern is obtained that resembles the real fractals.
iii. To best describe the growth of complex geometric patterns in polymer membrane, three production rules have been chosen and they are: F[+FF]F[-FF]F, F[+FF]F, and F[-FF]F.

Figures 10(a) (i-v) present the fractals observed in the PEO-NH_4I membrane shown in Figure 8. Their patterns simulated using L-systems are shown in Figures 10(b) (i-v).

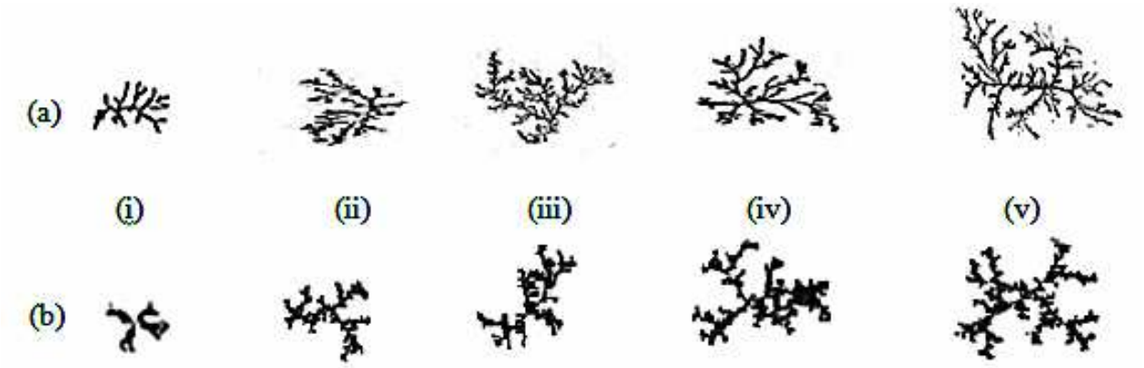


Fig. 10. The experimentally observed (a) and simulated (b) DLA patterns in PEO-NH_4I system using L-Systems

Table 3 gives the fractal dimensions for the original and simulated fractals. The table shows that the fractal dimension values of the simulated fractals are comparable with the fractal dimension values obtained from their respective experimentally cultured ones. For example, the fractal dimension of experimentally cultured fractal in Figure 10(a) (v) is 1.742 ± 0.044 while its corresponding simulated fractal, Figure 10(b) (v) has a fractal dimension of 1.751 ± 0.045. The error values for both experimentally and simulated patterns are found to be so small with standard deviation of less than 1.6%.

Experimentally cultured fractals		Simulated fractals using L-Systems		Percentage of difference (%)
Figure	Fractal dimension	Figure	Fractal dimension	
10(a)(i)	1.688 ± 0.049	10(b)(i)	1.645 ± 0.052	1.51
10(a)(ii)	1.719 ± 0.043	10(b)(ii)	1.756 ± 0.043	1.25
10(a)(iii)	1.754 ± 0.047	10(b)(iii)	1.737 ± 0.047	0.55
10(a)(iv)	1.706 ± 0.045	10(b)(iv)	1.761 ± 0.044	1.54
10(a)(v)	1.742 ± 0.044	10(b)(v)	1.751 ± 0.045	0.26

Table 3. Fractal dimension values of the fractals simulated using L-system and their respective experimentally cultured fractal patterns.

In the simulation using L-system technique, the branches grew completely one after the other from their nucleation center and thus making it difficult to get a complete full grown cluster that matched exactly as the experimentally cultured fractal patterns. These are among the factors which make it difficult to get absolute accuracy thus giving way to the small percentage differences of fractal dimension values between the experimental and simulated patterns.

5. Future research

Fujii et al. (1991) have studied the growth of fractal patterns in a conducting polymer. Furthermore, studies done by Shui et al. (2004) and Rosso (2007) have also gained significant

improvements toward the understanding of these phenomena. However the effects of such phenomena in secondary battery have not been fully understood. It is difficult to actually study directly the growth of fractal pattern that forms in the electrode since the fractal patterns could be easily damaged during accumulation. Thus as a substitute, fractals can be cultured in ion conducting polymer electrolyte membrane to replicate the condition in a similar environment via laboratory experiments. With this simple approach, study of the temporal images of the fractal growth pattern by utilizing a programmable image data acquisition device can also be done to get a more accurate simulation. For future research, extension of the basic DLA model or modifications on the L-systems can be carried out to get better results for the morphological evaluations of the fractal growth patterns. Then the dependence of the fractal dimension on the stages of growth can be evaluated and the effect of fractal dimension on the growth process in laboratory scale can further be investigated.

6. Conclusion

Many studies on fractals have been carried out either in applications, usually involving experimental works, or in theory, where most simulations on fractal patterns models are on nature-based fractals such as river flows, coastline and tree branching. This chapter focuses on the simulation of laboratory cultured fractals using ion conductive polymer electrolyte membranes as the media of growth. The simulation developed here is a DLA model based on the Brownian motion theory and a fractal dialect known as L-systems. A computer program has been developed to simulate and visualize the fractal growth. This computer program was also built to calculate the fractal dimension values of the simulated fractal patterns. Comparisons of the fractal dimension values between the laboratory cultured and the simulated fractals indicate an acceptable conformity with each other.

7. Acknowledgment

The authors would like to express gratitude and sincere appreciation to all the individuals whom directly and/ or indirectly helped realized the success of this research work. Financial support given by the University of Malaya, in terms of Short Term Research Funds (FP007/2005D and FS123/2008B) is greatly acknowledged.

8. References

Abelson, H. & diSessa, A. A., (1982) *Turtle geometry*. M.I.T. Press, Cambridge.

Addison, Paul S., (1997) *Fractals and Chaos - An Illustrated Course*. Institute of Physics (IoP) Publishing

Aharony, A., (1991), in: *Fractals and Disordered Systems,* ed. by Bunde, A. & Havlin, S.: Springer, p.177-178.

Alfonseca, M. & Ortega, A. (2001)*Determination of fractal dimensions from equivalent L systems* IBM J. RES. & DEV. 45**,** 6, 797-850.

Amir, S., Mohamed, N. S. & Hashim Ali, S. A. (2010a) *Cent. Eur. J. Phys.* Vol. 8(1) pp. 150-156

Amir, S., Mohamed, N. S., Subban, R. H. Y. (2010b) 'The Investigation on Ionic Conduction of PEMA Based Solid Polymer Electrolytes', *Advanced Materials Research* 93 - 94 381-384

Amir, S., Mohamed, N.S. & Hashim Ali, S. A. (2010c) Using Polymer Electrolyte Membranes as Media to Culture Fractals: A Simulation Study, *Advance Materials Research,* 93-94 35-38

Amir, S, Hashim Ali, S. A. & Mohamed, N. S. (2011a) Studies of fractal growth patterns in poly (ethylene oxide) and chitosan membranes. *Ionics*. 17(2) 121-125.

Amir, S. Hashim Ali, S. A. & Mohamed, N. S. (2011b). Ion Conductive Polymer Electrolyte Membranes and Simulation of Their Fractal Growth Patterns. *Sains Malaysiana* 40(1) 75-78

Armand, M.B, Chabagno, J.M. and Duclot, M.J. (1979), in: Fast Ion Transport in Solids, (eds.) Vashita, P., Mundy, J.N. and Shenoy, G.K., Elseiver North-Holland, New York, 131

Barkey, D., (1991). *J. Electrochem. Soc.* 138: 2912.

Ben-Jacob, E., Shochet, O., Tenenbaum, A., Cohen, I., Czirok, A. & Vicsek, T. (1994). *Nature* 368, 46.

Borghini, M.C., Mastragostino, M. and Zanelli, A. (1996), 'Investigation on lithium/polymer electrolyte interface for high performance lithium rechargeable batteries', *J. of Power Sources* 68 52-58

Broadbent, S. R. & Hammersley, J.M. (1957). Percolation Process I. Crystals and Mazes. *Proc. Cambridge Philos. Soc*. 53, 629-641.

Carr, B.J. & Coley, A.A. (2003). Self-similarity in general relativity, Available from http://users.math.uni-potsdam.de/~oeitner/QUELLEN/ZUMCHAOS/ selfsim1.htm

Chandra, A. & Chandra, S. (1994) *Physical Review B*. *The American Physical Society* 49, 1, pp. 633-636

Chandra, A. (1996) *Solid State Ionics* 86-88 , pp. 1437-1442

Chandra, A. & Chandra, S. (1993). *Current Sci*. 64, pp. 755.

Chen, J.-D. & Wilkinson, D. (1985). Pore-scale viscous fingering in porous media. *Phys. Rev. Lett.*, pp. 1892-1895.

Combes, F. (1998). Fractal Structures Driven by Self-gravity: Molecular Clouds and the Universe. *Springer* 72, pp. 1-2.

Cross SS. (1997). Fractals in pathology. *J Pathol* 182, pp. 1−8.

Dargahi-Noubary, G. R. (1997). A Test of the Cyclicity of Earthquakes, *Natural Hazards* 16 pp. 127–134.

Deering, W. & West, B.J. (1992). Fractal Physiology. *IEEE Engin. Med. Biol*. 11, pp. 40-46.

Dierking, I. (2000). Fractal Growth of the Liquid Crystalline B2 Phase of a Bent-core Mesogen. *J. Phys*:C:*Condens. Matter.* 13, pp. 1353-1360.

Ebert, D. S.(1996). Advanced Modeling Techniques for Computer Graphics, *ACM Computing Surveys*, 28(1), pp. 153-156.

Eden, M., (1961). *Proc. 4th Berkeley Symp. on Math. Stat. and Prob.* 4, pp. 223.

Family, F. & Vicsek, T., (1985), *J. Phys. A: Math. Gen*.18, pp. L75.

Family, F., (1990). *Physica A* 168, pp. 561

Feder, J.(1988). *Fractals*, New York: Plenum Press.

Focardi, S.M. (2003). Fat tails, scaling and stable laws: A critical look at modeling extremal events in economic and financial phenomena, Available from http://www.theintertekgroup.com/scaling.pdf

Fujii, M.; Arii, K. & Yoshino, K. (1991). The Growth of Dendrites of Fractal Pattern on a Conducting Polymer. *J. Phys.: Condens. Matter*, 3, pp. 7207-7211

Golubev, Yu. N., Fomin, V. V. & Cherkesov, L. V. (1987). Interaction between surface gravitational waves and local rise of sea-bed in the uniform ocean, Physical Oceanography, *Springer New York*, 1, 1, pp. 3-9.

Hashim Ali, S. A.; Mohamed, N. S.; Shariff, A. A. & Arof, A. K. (2000). Simulating fractal growth in chitosan doped silver nitrate film using L-system, *Solidstate Ionic Devices: Science & Technology*, pp. 16-19

Hastings, H.O. & Sugihara, G.(1993). *Fractals: A Users Guide For The Natural Science*, New York: Oxford University Press.

Horvath, V. K., Family, F. & Vicsek, T., (1991). *Phys. Rev. Lett.* 67, pp. 3207.

Janke, W. & Schakel, A. M. J. (2005). *Phys. Rev. Lett.* 95, pp. 135702

Judd, C.(2003). Fractals – Self-Similarity, 17.06.2007 Available from http://www.bath.ac.uk/~ma0cmj/FractalContents.html

Kaandorp, J.A. (1994). *Fractal modelling: growth and form in biology.* Springer-Verlag, Berlin, New York.

Kaufmann, J. H., Nazzal, A. I. & Melroy, O. R. (1987). *Phys. Rev. B* 35, pp. 1881-1890.

Kenkel, N.C. & D.J. Walker. (1993). Fractals and ecology. *Abst. Bot.* 17,pp. 53-70.

Lindenmayer, A. (1968)."Mathematical models for cellular interaction in development." *J. Theoret. Biology,* 18, pp. 280-315.

Lo Verso, F.; Vink, R. L. C.; Pini, D. & Reatto, L. (2006). *Physical Review E* 73, pp. 061407

Loehle, C. (1983). The fractal dimension and ecology. *Specul. Sci. Tech.* 6, pp. 131-142.

Maloy, K.J., Feder, J. & Jossang, T. (1985). *Phys. Rev. Lett.* 55, pp. 2688.

Mandelbrot, B. B. (1983). *The Fractal Geometry of Nature*, San Francisco: W. H. Freeman and Co.

Mandelbrot, B., (1977). *Fractals: Form, Chance and Dimension*,; W H Freeman and Co.

Marcone, B.; Orlandini, E. & Stella, A. L. (2007). Knot localization in adsorbing polymer rings, *Physical Review E* 76, pp. 051804

Matsushita, M., Sano, M., Hayakawa, Y., Honjo, H. & Sawada, Y. (1984). *Phys. Rev. Lett.* 53, pp. 286.

Matsuura, S. & Miyazima, S. (1992). *Physica A* 191, pp. 30.

Matsuyama, T., Harshey, R. M. & Matshushita, M.(1993). *Fractals* 1, pp. 336.

Murata, K. (1995), 'An overview of the research and development of solid polymer electrolyte batteries', *Electrochim. Acta* 40 2177-2184

McNamee, J. E. (1991) Fractal Perspectives in Pulmonary Physiology. *J. Appl. Physiol.* 71(1), pp. 1-8.

Meakin, P. (1988),Simple Models for Crack Growth, *Crystal Prop.* Prep.*17* and*18*, pp. 1–54.

Meakin, P. (1991), Models for Material Failure and Deformation, *Science252*, pp. 226–234.

Musgrave, F. K., (1993). *Methods for Realistic Landscape Imaging*, Yale University

Niemeyer, L., Pietronero, L.& Wiesmann, H.J. (1984). *Phys. Rev. Lett.* 52, pp. 1033 -1036

Okubo, S., Mogi, I., Kido, G. & Nakagawa, Y. (1993). *Fractals* 1, pp. 425.

Ouellette, J.,(2001)Pollock'sFractals, 27.10.2007, Available from http://discovermagazine.com/2001/nov/featpollock

Papert, S.(1980). *Mindstorms: Children, Computers, and Powerful Ideas.* Basic Books, New York,

Peitgen , H.O. & Saupe, D.(1988). *The Science of Fractal Images*, Berlin: Springer-Verlag.

Peitgen , H.O., Jurgens, H. & Saupe, D.(1992). *Fractals for the Classroom*, New York: Springer-Verlag.

Prusinkiewicz P. (1986). *Graphical applications of L-systems*. Proceedings Graphics

Prusinkiewicz, P. & Lindenmayer, A. (1990). *The Algorithmic Beauty of Plants*. Springer-Verlag, New York.

Radnoczy, G., Vicsek, T, Sander, L.M. & Grier, D. (1987). *Phys.Rev A* 35, pp. 4012

Rathgeber, S.; Monkenbusch, M.; Hedrick, J. L.; Trollsås, M. & Gast, A. P. (2006). *J. Chem. Phys.* 125, pp. 204908

Ratner, M.A. (1987), in 'Polymer Electrolyte Reviews I, Ed. J.R. MacCallum and C.A. Vincent, Elseiver Applied Science, London, 173-236

Rosso, M. (2007) *Electrochimica Acta* 53 250–256

Rucker, R. (1984), *The Fourth Dimension*, Houghton-Mifflin

Saffman P. G. & Taylor G., (1958). The penetration of a fluid into a medium of hele-shaw cell containing a more viscous liquid. *Proc. Soc. London, Ser A,* pp. 312-329.

Sawada, Y., Dougherty, A., Gollub, J.P. (1986): *Phys. Rev. Lett.* 56, pp. 1260.

Shibkov, A. A., Golovin Yu. I., Zheltov, M. A., Korolev A. A. & Vlasov A. A., (2001). Kinetics and morphology of nonequilibrium growth of ice in supercooled water, *Crystallography Reports*, 46, 3, pp. 496-502.

Shui, J.L., Jiang, G.S. Xie, S. & Chen, C.H. (2004) *Electrochimica Acta* 49 2209–2213

Sławinski, C., Sokołowska, Z. Walczak, R., Borówko, M. & Sokołowski, S. (2002). Fractal dimension of peat soils from adsorption and from water retention experiments, *Colloids and Surfaces, A: Physicochemical and Engineering Aspects* 208, pp. 289–301.

Smith Jr. T.G., Marks W.B., Lange G.D., Sheriff Jr. W.H. & Neale E.A. (1990). A fractal analysis of cell images. *J.Neurosci.Meth.* 27, pp. 173-180.

Stanley, H. E. , Buldyrev, S. V. , Goldberger, A. L. , Havlin S. , Mantegna, R. N. , Ossadnik, S. M., Peng, C. -K. , Sciortino, F. & Simons, M.(1994). *Fractals in Biology and Medicine: Lecture notes in Physics*. USA:Springer .

Suki, M.N.; Mohamed, N.S.; Hashim Ali, S.A. & Zainuddin, R. (2007). The role of image processing in measuring fractal dimension, *Malaysian Journal of Science*, pp. 23-33

Tordoff, G. M. Boddy, L. & Hefin Jones, T.(2007), Species-specific impacts of collembola grazing on fungal foraging ecology, *Soil Biology & Biochemistry*, pp. 1-9.

Vicsek, T. (1992) *Fractal Growth Phenomena*, second edition World Scientific Publishing

Villani, V. and Comenges, J. M. Z.(2000). Analysis of biomolecular chaos in aqueous solution. *Springer* 104, pp. 3-4.

West, B.J. & A.L. Goldberger.(1987). Physiology in fractal dimensions. *Am. Sci*. 75, pp. 354-365.

Wiens, J.A. (1989). Spatial scaling in ecology. *Funct. Ecol.* 3, pp. 385-397.

Witten Jr, T. A. & Sander, L. M. (1981). *Phys. Rev. Lett.* 47, pp. 1400.

Yadegari, S., Self-similarity, 16.03.2007, Available from http://www.crca.ucsd.edu/~syadegar/MasterThesis/node25.html

Zhang, G., Jin, L., Ma, Z., Zhai, X., Yang, M., Zheng, P., Wang, W. & Wegner, G. (2008). *J. Chem. Phys.* 129, pp. 224708

INTECH
open science | open minds

InTech Europe
University Campus STeP Ri
Slavka Krautzeka 83/A
51000 Rijeka, Croatia
Phone: +385 (51) 770 447
Fax: +385 (51) 686 166
www.intechopen.com

InTech China
Unit 405, Office Block, Hotel Equatorial Shanghai
No.65, Yan An Road (West), Shanghai, 200040, China
中国上海市延安西路65号上海国际贵都大饭店办公楼405单元
Phone: +86-21-62489820
Fax: +86-21-62489821

IntechOpen

IntechOpen

© 2012 The Author(s). Licensee IntechOpen. This is an open access article distributed under the terms of the Creative Commons Attribution 3.0 License, which permits unrestricted use, distribution, and reproduction in any medium, provided the original work is properly cited.

IntechOpen

IntechOpen